JOURNAL OF CHEMICAL INFORMATION AND MODELING

Article

pubs.acs.org/jcim

Discovery and Design of Tricyclic Scaffolds as Protein Kinase CK2 (CK2) Inhibitors through a Combination of Shape-Based Virtual Screening and Structure-Based Molecular Modification

Haopeng Sun,[†,‡,§] Xiaoli Xu,[†,‡] Xiaowen Wu,[†,‡] Xiaojin Zhang,*[,†,‡,∥] Fang Liu,[†,‡] Jianmin Jia,[†,‡] Xiaoke Guo,[†,‡] Jingjie Huang,[†,‡] Zhengyu Jiang,[†,‡] Taotao Feng,[†,‡] Hongxi Chu,[†,‡] You Zhou,[†,‡] Shenglie Zhang,[†,‡] Zongliang Liu,*[,⊥] and Qidong You*[,†,‡]

[†]State Key Laboratory of Natural Medicines, China Pharmaceutical University, Nanjing 210009, China

[‡]Jiangsu Key Laboratory of Drug Design and Optimization, China Pharmaceutical University, Nanjing 210009, China

[§]Department of Medicinal Chemistry, School of Pharmacy, China Pharmaceutical University, Nanjing 210009, China

[∥]Department of Organic Chemistry, School of Science, China Pharmaceutical University, Nanjing 210009, China

[⊥]School of Pharmacy, Yantai University, Yantai 264005, China

Supporting Information

ABSTRACT: Protein kinase CK2 (CK2), a ubiquitous serine/threonine protein kinase for hundreds of endogenous substrates, serves as an attractive anticancer target. One of its most potent inhibitors, CX-4945, has entered a phase I clinical trial. Herein we present an integrated workflow combining shape-based virtual screening for the identification of novel CK2 inhibitors. A shape-based model derived from CX-4945 was built, and the subsequent virtual screening led to the identification of several novel scaffolds with high shape similarity to that of CX-4945. Among them two tricyclic scaffolds named [1,2,4]triazolo[4,3-c]quinazolin and [1,2,4]triazolo-[4,3-a]quinoxalin attracted us the most. Combining strictly chemical similarity analysis, a second-round shape-based screening was performed based on the two tricyclic scaffolds, leading to 28 derivatives. These compounds not only targeted CK2 with potent and dose-dependent activities but also showed acceptable antiproliferative effects against a series of cancer cell lines. Our workflow supplies a high efficient strategy in the identification of novel CK2 inhibitors. Compounds reported here can serve as ideal leads for further modifications.

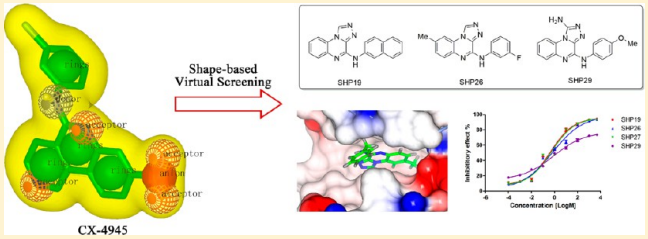

INTRODUCTION

Protein kinase CK2 (CK2) is a highly pleiotropic and conserved serine/threonine kinase that plays key roles in cell growth, proliferation, and survival.[1,2] Over 300 protein substrates of CK2 have already been identified.[3] CK2 typically forms a tetrameric complex consisting of two catalytic α subunits (α or α') and two regulatory β subunits in various combinations.[4] The CK2α subtype has been reported to be ubiquitous, while the CK2α' subtype is exclusively located in the brain and testis.[5] Only until recently it has been considered as a promising target in cancer chemotherapy.[6] It has been well demonstrated that the overexpressed CK2 is closely related to a number of cancers, including head and neck,[7] breast,[8,9] colorectal,[10] renal,[11] lung,[12] leukemias,[13] and prostate.[14] Compared to other signaling kinases, CK2 has several specific advantages, including the following: (1) CK2 is reported to be constitutively active under normal conditions and does not need the specific stimuli.[15] (2) Unlike other kinases, where genetic alterations lead to dysregulation of their pathways, no CK2 mutations have been identified so far, indicating more stable therapeutic effects of the inhibitors.[16,17] (3) The ATP binding site of CK2 is smaller than most of the other kinases due to the presence of unique bulky residues such as Val 66 and Ile174, allowing for the design of very selective low molecular weight ATP-competitive inhibitors.[18]

Till now, there are several series of CK2 inhibitors reported (Figure 1). The chlorinated nucleoside **1** (DRB, IC_{50} = 15 μM) was one of the earliest identified inhibitors of CK2.[19] Natural products such as emodin **2** (IC_{50} = 2 μM),[20] apigenin **3** (IC_{50} = 0.8 μM),[21] and ellagic acid **4** (IC_{50} = 0.04 μM)[22] displayed greater potency but generally lacked specificity. Inhibitors containing the tetrabromobenzimidazole core, such as TBB **5**,[23−26] have been proved to have higher selectivity and potency. These compounds have been widely used as molecular probes to elucidate the functional role of CK2. Although well tolerated in mice,[27] the polyhalogenated aromatic nature of **5** and its analogues is prone to raise potential long-term toxicity in humans, which hindered the clinical trial.[28] Another potent and selective inhibitor **6** (IQA, IC_{50} = 80 nM)[29] was discovered by utilizing high throughput docking methodologies. However, **6**

Received: February 18, 2013
Published: July 16, 2013

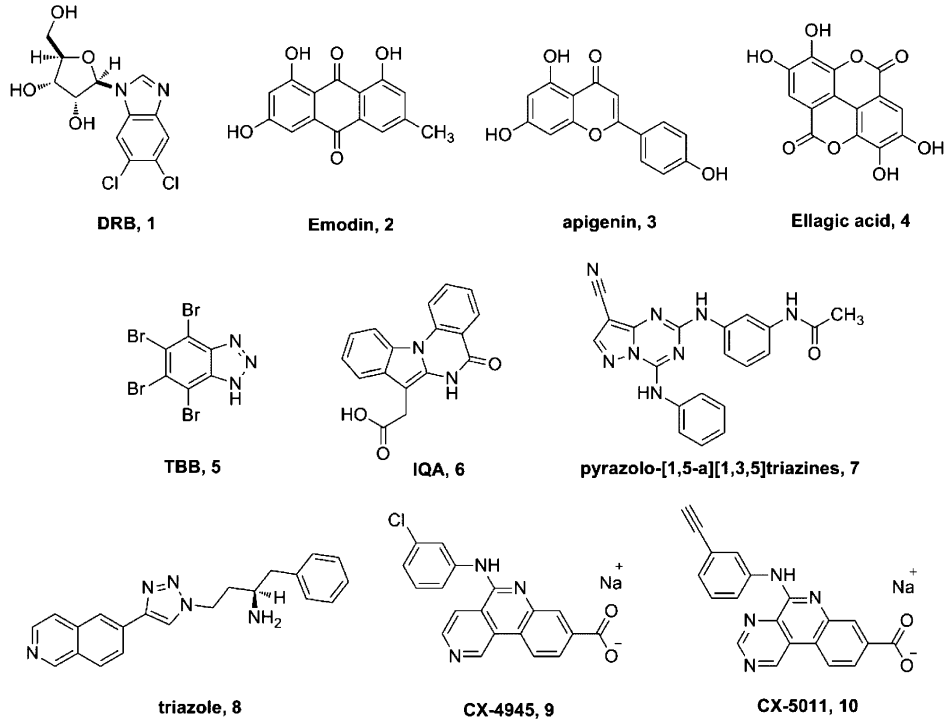

Figure 1. Representative structures of known inhibitors of CK2.

was reported to decompose slowly in aqueous media, precluding its use as a drug.[30] A novel pyrazolo[1,5-a][1,3,5]triazines compound **7** and its derivatives emerged as a potent class of CK2 inhibitors. Several analogues were reported to have the K_i values of below 1 nM[31,32] and demonstrated cellular antiproliferative activity in the submicromolar range. However, the current status of these noteworthy molecules remains undisclosed. A recent publication described the discovery and cellular characterization of a novel molecule **8**, which induced antiproliferative responses in cell culture, by inhibiting the phosphorylation of the CK2 substrate PTENat Ser 370.[33] The possibility of design modulators targeting the allosteric site of CK2 was also discussed by Prudent et al.,[34] pointing out the novel molecular design strategy of CK2 inhibitors.

As mentioned above, most of the available molecules lack the potency, physiochemical, and pharmacological properties required to be successful in a clinical setting. The need for new classes of CK2 inhibitors satisfying these challenges is clear. Among the inhibitors available for this kinase, the recently developed **9** (CX-4945)[35] and **10** (CX-5011)[36] (Figure 1) have been demonstrated to be very potent, effective, and selective in inducing cell death in tumor cells. As an ideal lead, CX-4945 has recently entered clinical trials according to Cylene's report.[37] The exciting data clearly indicate the therapeutic potential of novel CK2 inhibitors.

Ligand-based virtual screening of large compound databases has been proved to be an effective method in discovering novel hits for a certain target.[38−40] The knowledge-driven approach helps medicinal chemists to optimize active chemical scaffolds, leading to novel active compounds. Among all the ligand-based approaches, the qualitative (e.g., Hiphop model[41]) or quantitive (e.g., Hypogen model[42]) common structure pharmacophore might be the most successful and popular models. The pharmacophore is a set of chemical features aligned in three-dimensional (3D) space. The spatial arrangement of chemical features represents the essential interactions between proteins and ligands.[43] However, this method closely depends on the training set selection during the model construction. The resulting models always emphasize the common structural information too much, negelecting the unique characters of a given target, such as spatial volume requirements and physicochemical properties. Additionally, the experience of the researchers also deeply affects the accuracy and reliability of the models.

To avoid these problems, we first built a virtual screening model on the basis of CX-4945 by using OMEGA/ROCS[44,45] software packages from OpenEye (www.eyesopen.com). Rapid Overlay of Chemical Structures (ROCS) uses an alignment algorithm accounting shape/physicochemical properties for the query molecule orientation.[46] The model was then applied to virtually screen the Topscience (www.tsbiochem.com) database, resulting in several novel scaffolds with high shape similarity to that of CX-4945. Among them a tricyclic scaffold named [1,2,4]triazolo[4,3-c]quinazolin (**SHP01**) attracted us the most. We then selected **SHP01** to generate the ROCS model. Combining strictly chemical similarity analysis, a second-round shape-based screening was performed. Twenty-eight derivatives with two scaffolds, named [1,2,4]triazolo[4,3-c]quinazolin and [1,2,4]triazolo[4,3-a]quinoxalin (**SHP02−SHP29**) were finally retained and purchased from Topscience. They were evaluated for their anti-CK2 and antiproliferative activity in multiple cancer cell lines. Figure 2 shows a graphical summary of the workflow.

RESULTS AND DISCUSSIONS

ROCS Model Generation Based on CX-4945 and Virtual Screening. CX-4945 was selected as the reference molecule to generate the ROCS model. The algorithm is based on the idea that if the molecules overlay well, the molecular shapes of the compounds are similar. Besides, any volume mismatch is resulting from shape dissimilarity.[47] A smooth Gaussian function is applied to represent the molecular volume while superimposing the molecules. The overlay of the molecules is then

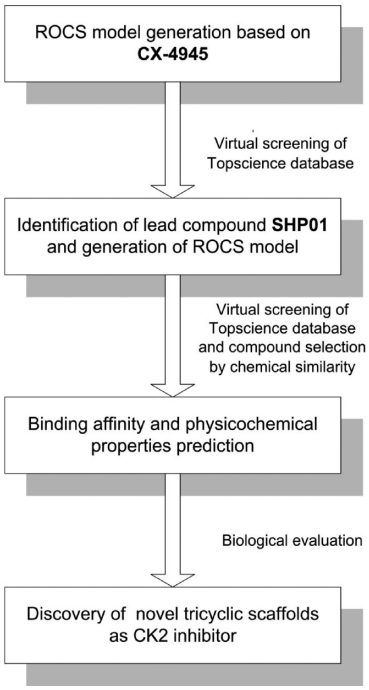

Figure 2. Overview of the molecular modeling workflow.

corrected and evaluated by simple matching of chemical functionalities.[48] A recent study suggests that the bioactive conformation of a reference molecule is not needed for the enrichment of shape based screening.[49] These findings encouraged us to employ this complementary methodology as a screening model for the identification of novel scaffolds that possess similar structures with CX-4945. The 3D shape-based similarity of a given compound to CX-4945 was ranked by a combined scoring method. It consisted of the shape Tanimoto coefficient and the score retrieved from the ROCS color force field, which included rough information about chemical functions. As both scores vary from 0 to 1, the combo score as the sum of both varies between 0 and 2.[50] The structure of CX-4945 was separated from the cocrystal complex (PDB id: 3PE1) and further minimized using Discovery Studio (DS) with a CHARMm forcefield. Then the molecule was directly used to generate the ROCS query. The key scaffold of CX-4945 was defined by its polycyclic core. The polar atoms such as the nitrogen of pyridine and the amino group were defined as hydrogen bond acceptor and donor, respectively. The carboxyl group was described by an anion feature in complex with two hydrogen bond acceptors. The molecular shape of CX-4945 was depicted in a yellow shadow (Figure 3B). The ROCS model was quite in accordance with the binding pattern revealed by the cocrystal structure (Figure 3A). The nitrogen atoms on a pyridine ring and an amino group formed an H-bond with H_2O 471 and H_2O 475, respectively. The carboxyl group of CX-4945 served as a strong polar contact group with CK2, forming four H-bonds with Lys68, Asp175, H_2O 416, and H_2O 427, respectively. Such consistency showed that our model contained the key features that played a significant role while interacting with CK2. Further exploration of the database using the model will lead to the compounds with similar chemical property and molecular shape to CX-4945.

Identification of the Lead Compound SHP01 and Its Derivatives by Using ROCS Model and Chemical Similarity Search. For the Topscience database, the multiple conformations of different query molecules were calculated using OMEGA (default settings, with a maximum of 400 conformations per molecule). In the subsequently performed shape-based similarity screening, the query molecules were ranked by the combo score. The scored hit list was visually inspected, and 13 compounds were chosen for biological testing. The selection was based on two criteria: (i) compounds were available at the time of our study and (ii) showed sufficient structural diversity among each other. Among them 8 compounds show over 50% activity inhibition against CK2 under 10 μM (one is the lead compound **SHP01** represented here, other structures are not reported here). The exciting result encouraged us a great deal and showed the reliability of the ROCS model in the identification of novel scaffolds as CK2 inhibitors.

The binding pattern of **SHP01** with CK2 was analyzed by molecular docking. The compound inserted well into the active site of CK2. Two hydrogen bonds were detected: one was from the nitrogen atom on the triazole ring to Glu114, a residue in the hinge region of the active site; another was between the nitrogen

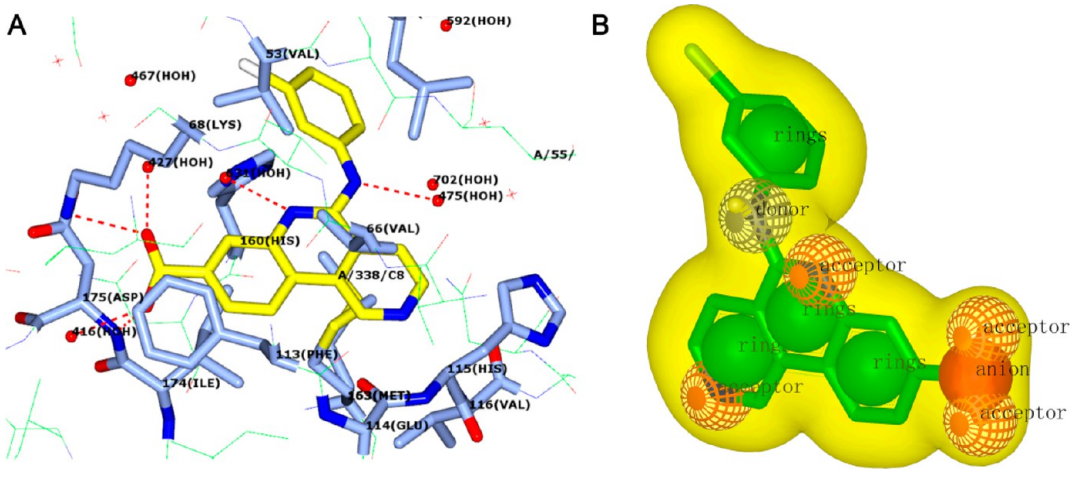

Figure 3. The binding pattern of CX-4945 with CK2 (A) and the ROCS model (B). The binding pattern was generated from the cocrystal structure (PDB id: 3PE1) depicted using the CCP4MG program (www.ccp4.ac.uk). The carbon atoms of CX-4945 and the key residues in the active site of CK2 were colored in yellow and ice blue cylinders, respectively. The H-bonds were shown as red dot lines. For the display of the ROCS model of CX-4945, the carbon atoms were shown as green and the molecular shape was visualized as a yellow shadow.

dx.doi.org/10.1021/ci400114f | J. Chem. Inf. Model. 2013, 53, 2093−2102

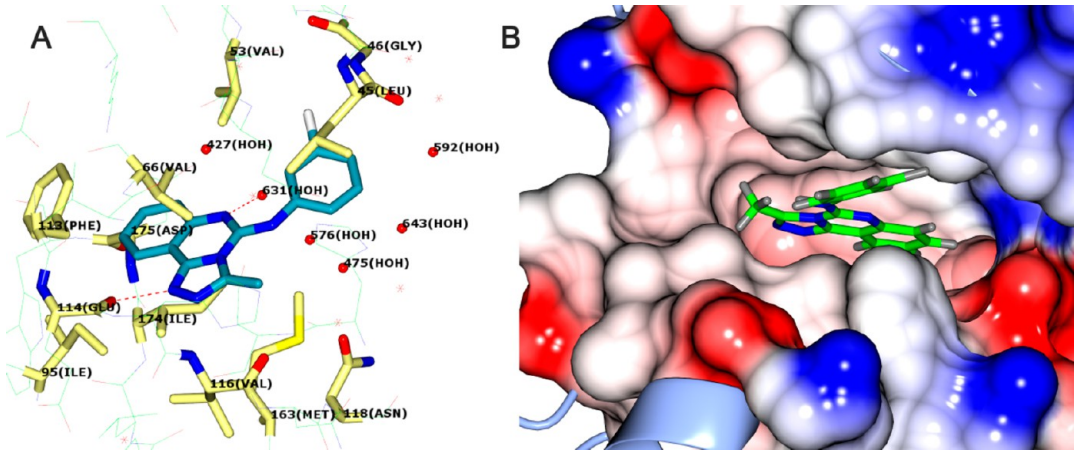

Figure 4. The binding pattern of **SHP01** with CK2. The interaction mode was obtained through molecular docking (PDB id: 3PE1) and depicted using the CCP4MG program. The key residues (A) and the protein surface (B) around **SHP01** were shown, respectively. The carbon atoms of CX-4945 and the key residues in the active site of CK2 were colored in ice blue and golden cylinders, respectively. The surface was colored by the electrostatic state of the residues.

atom on the pyrimidine ring and an active water molecule. The tricylic scaffold of **SHP01** was surrounded by the steric and hydrophobic residues such as Val66, Ile95, Phe113, and Ile174 (Figure 4A). The binding pattern was also depicted by the 'surface around ligand' mode in the CCP4MG program. It can be easily observed that **SHP01** occupied the active cavity well in a reasonable conformation (Figure 4B). The tricylic scaffold was deeply buried into the surface of the key residues, while the phenylamine pointed to an open area at the edge of the active site. The binding mode analysis clearly explains the activity of **SHP01** and indicates that the compound can serve as a proper lead compound.

In order to expand the chemical diversity, researchers are always prone to retain compounds with different scaffolds during virtual screening. As for compounds with similar structures, they usually pick one as the representative. However, there are some problems in using such a representative. First, the information obtained from single compound is not enough to describe the character of the target binding site and reveal the key interactions. Under such circumstances, medicinal chemists carry out the structural modification only by their experience. Such modification is usually unreasonable and time-consuming, thus reducing the efficiency of the research. Second, it is equivocal to determine the activity of a chemical scaffold judging by one compound because of the potential experimental error, which may bring the deviation in the subsequent molecular design. To solve these problems and confirm the activity of screening hits, we further performed a chemical similarity search based on **SHP01**. A ROCS model was generated on the basis of the structure of **SHP01**; 500 compounds with similar molecular shape to **SHP01** were screened out. The structural similarity was later analyzed using these molecules which were then analyzed using Functional-Class Fingerprints_6 (FCFP_6)[51,52] molecular fingerprint. Compounds with a Tanimoto coefficient over 0.5 were recognized as similar structures to **SHP01**. After such screening, 28 commercial available derivatives of **SHP01** were retained and processed to bioevaluation (Table 1). They can be divided into two series: [1,2,4]triazolo[4,3-c]quinazolin (scaffold A) and [1,2,4]triazolo[4,3-a]quinoxalin series (scaffold B). All the compounds can be purchased from the Topscience database.

The inhibitory IC_{50} against CK2 were determined using the CK2 assay kit. Structure−Activity Relationship (SAR) analyses of the identified compounds were carried out based on the biological data. Compounds with scaffold A showed moderate inhibitory effects on CK2. Among these compounds, small substituted groups at the R_1 position could slightly improve the activity (e.g., **SHP08** vs **SHP11**), indicating steric groups were not preferable at this position. For R_2 substitution, the decreased activities of **SHP06** and **SHP07**, compared to other compounds, suggested aromatic rings were preferred. Phenyl with 3- or 4-substitutions could enhance the activities, while 2-substitutions obviously decreased the activities (e.g., **SHP01**, **SHP03** vs **SHP02**, **SHP04** vs **SHP05**). This can be explained by the unpleasant intermolecular repulsion to Leu45 and Val53 (Figure 4).

Compounds with scaffold B (**SHP12**-**SHP29**) showed much improved activities compared to compounds with scaffold A. For the R_1 group, it clearly shown that small groups were preferred at this position. Compounds with methyl or ethyl at this position were less active than those compounds with hydrogen substitution (e.g., **SHP12** vs **SHP27**, **SHP15** vs **SHP18**). A polar group such as amino (**SHP29**) also enhanced the activity, with IC_{50} 0.87 ± 0.10 μM (Figure 5), thus polar contacts at this position may improve the binding affinity. For the R_2 group, the aromatic ring with steric groups dramatically improved the inhibitory activities. It was worth noticing that **SHP19** with naphthalen-2-yl at the R_2 position exhibited the most potent activity among all the compounds, with IC_{50} 0.46 ± 0.08 μM (Figure 5). The data indicated that the aromatic ring at the R_2 position inserted into a hydrophobic pocket of CK2. For the R_3 group, substitution with small groups such as methyl or chlorine obviously enhanced the inhibitory effects, and **SHP26** and **SHP27** showed submicromolar inhibitory IC_{50} 0.69 ± 0.06 and 0.55 ± 0.08 μM (Figure 5), respectively. The data suggested that rational optimization at R_3 may generate more potent compounds.

We next analyzed the binding modes between the active compounds (**SHP19**, **SHP26**, and **SHP29**) and the binding site of CK2 by molecular docking (Figure 6). The tricyclic scaffold inserted into the small and hydrophobic binding pocket P1, which was buried deeply in CK2. The hydrophobic contact decreased the binding free energy, forming a stable intermolecular interaction. Another binding pocket adjacent to P1, named P2, was observed to be mainly occupied by R_2 groups.

dx.doi.org/10.1021/ci400114f | J. Chem. Inf. Model. 2013, 53, 2093−2102

Table 1. CK2 Inhibitory Activity, Binding Affinity Prediction, and Physicochemical Properties Calculation of the Screened out Compounds

Scaffold

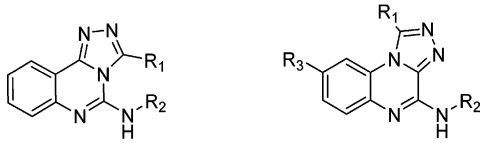

A B

scaffold	ID	R1	R2	R3	CK2 inhibitory IC_{50}, μM	combo score	CLogP
A	**SHP01**	Me	3-chlorophenyl	-	4.23 ± 0.68	-	2.83
A	**SHP02**	Me	2-chlorophenyl	-	65.41 ± 8.34	1.86	2.83
A	**SHP03**	Me	4-chlorophenyl	-	15.41 ± 1.15	1.86	2.83
A	**SHP04**	Me	2-bromophenyl	-	71.45 ± 9.33	1.86	2.99
A	**SHP05**	Me	4-bromophenyl	-	7.35 ± 1.76	1.86	2.99
A	**SHP06**	Me	2-(cyclohex-1-en-1-yl)ethyl	-	38.84 ± 0.33	1.73	2.33
A	**SHP07**	Me	cyclooctyl	-	58.66 ± 7.89	1.78	2.94
A	**SHP08**	Me	4-morpholinophenyl	-	29.22 ± 1.93	1.71	2.11
A	**SHP09**	ethyl	2-fluorophenyl	-	77.05 ± 6.58	1.91	3.07
A	**SHP10**	ethyl	3-fluorophenyl	-	31.02 ± 2.66	1.93	3.07
A	**SHP11**	H	4-morpholinophenyl	-	24.17 ± 2.95	1.78	1.99
B	**SHP12**	Me	4-chlorophenyl	H	26.54 ± 4.39	1.82	2.75
B	**SHP13**	Me	2-chlorophenyl	H	36.54 ± 4.39	1.81	2.75
B	**SHP14**	Me	4-bromophenyl	H	7.47 ± 1.78	1.81	2.91
B	**SHP15**	Me	2-bromophenyl	H	10.56 ± 1.94	1.81	2.91
B	**SHP16**	Me	N,N-dimethylbenzenamine	H	1.61 ± 0.25	1.67	2.25
B	**SHP17**	Me	phenethyl	H	1.35 ± 0.22	1.55	2.79
B	**SHP18**	H	2-bromophenyl	H	2.27 ± 0.41	1.83	2.79
B	**SHP19**	H	naphthalen-2-yl	H	0.46 ± 0.08	1.70	3.01
B	**SHP20**	H	naphthalen-1-yl	H	7.59 ± 0.84	1.64	3.01
B	**SHP21**	H	2-chlorobenzyl	H	3.64 ± 0.57	1.54	2.38
B	**SHP22**	H	4-(methylthio)benzyl	H	13.52 ± 2.11	1.55	2.41
B	**SHP23**	H	4-methylbenzyl	Me	5.41 ± 0.64	1.59	2.80
B	**SHP24**	H	benzyl	chloro	1.62 ± 0.20	1.50	2.38
B	**SHP25**	H	4-methylbenzyl	chloro	2.19 ± 0.29	1.49	2.90
B	**SHP26**	H	3-fluorobenzyl	Me	0.69 ± 0.06	1.55	2.43
B	**SHP27**	H	4-bromophenyl	Me	0.55 ± 0.08	1.74	2.19
B	**SHP28**	ethyl	2-fluorophenyl	H	4.92 ± 0.63	1.75	2.99
B	**SHP29**	amine	4-methoxyphenyl	H	0.87 ± 0.10	1.76	1.72
CX-4945 (positive control)					0.06 ± 0.01	-	3.42

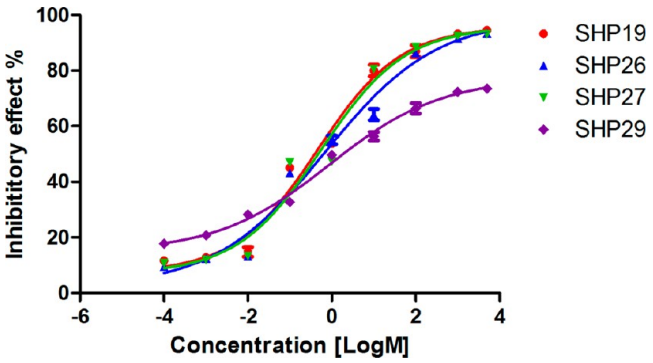

Figure 5. The biological evaluation of the potent compounds. The dose-dependent inhibitory manner of **SHP19**, **SHP26**, **SHP27**, and **SHP29**.

Compared to P1, P2 was a more large and flexible area on the edge of the surface of CK2. A small variation such as a halogen atom, methoxyl, or an amino group cannot obviously impact the binding affinity. As a result, different fragments can be introduced to R_2, optimizing the physicochemical properties of the compounds. Except for the hydrophobic contacts, the tricyclic ring also formed hydrogen bonds with the hinge region residues such as Glu114, Val 116, and His160. These hydrogen bonds improved the intermolecular recognition between the inhibitors and CK2, thus enhancing the binding affinity. For **SHP26**, the methyl at R_3 pointed to the polar region of CK2, which may cause improper interaction; therefore, this methyl could be substituted by polar groups that can interact with the polar residues. It was worth noticing the amino at the R_1 position of **SHP29** formed a hydrogen bond with Glu114, indicating that polar groups at this position can help bind to CK2. This can explain why hydrophobic groups such as methyl or ethyl decreased the activities.

We further tested the antiproliferative activities of the potent compounds in target-based evaluation (Table 2). Five cancer cell lines including A549, HepG2, HCT116, BxPC-3, and BT474 were tested using MTT assay. CX-4945 was used as positive control. The cell-based results indicated acceptable antiproliferative effects of our compounds. The most potent compound,

dx.doi.org/10.1021/ci400114f | J. Chem. Inf. Model. 2013, 53, 2093−2102

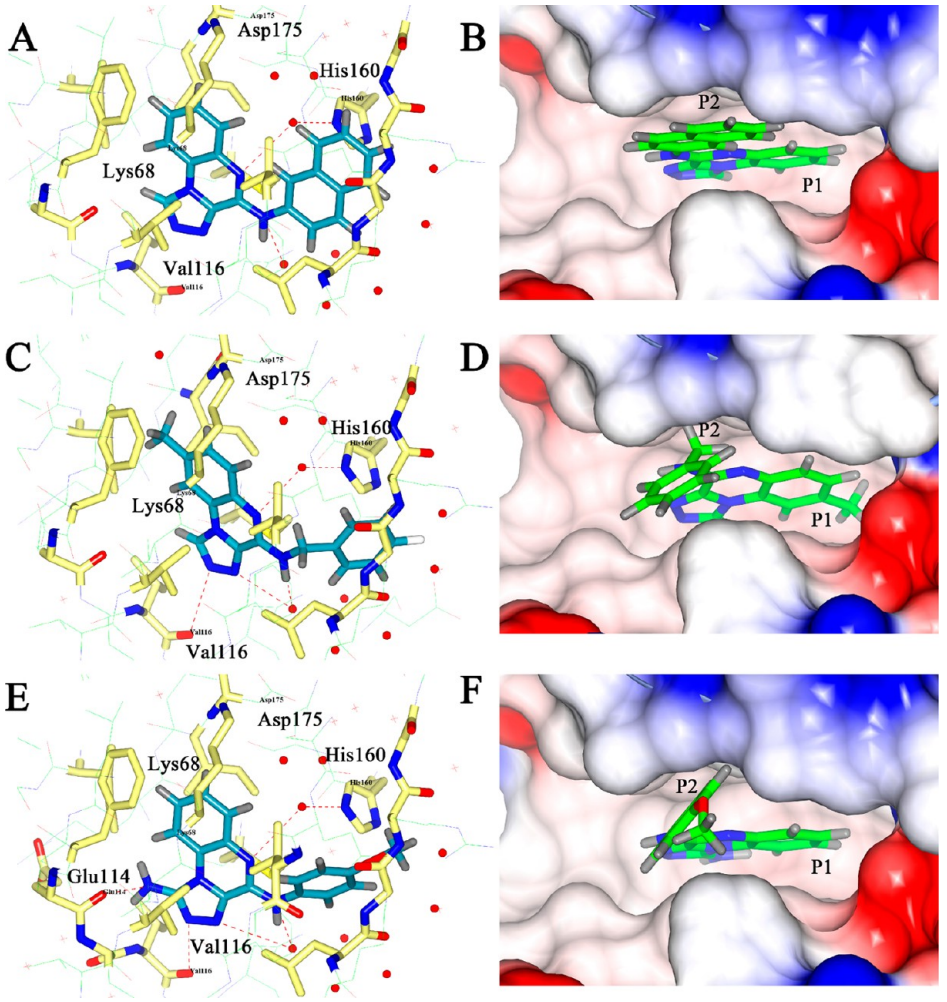

Figure 6. The binding pattern analysis of compounds **SHP19** (A, B), **SHP26** (C, D), and **SHP29** (E, F) to CK2. Gold 5.1 was used to carry out the molecular docking, and the data were displayed with CCP4MG. Compounds were shown as cylinders with carbon atoms colored in green. The electrostatic potential surface was added to the active site around the compounds.

Table 2. Cell Antiproliferative Activity of Derivatives for the Screened out Compounds

	cell viability IC_{50}, μM				
ID	A549	HepG2	HCT116	BxPC-3	BT474
SHP19	88.56 ± 13.24	57.09 ± 4.54	80.43 ± 6.55	40.70 ± 6.55	13.4 ± 1.57
SHP21	36.75 ± 3.13	57.34 ± 3.22	88.4 ± 7.01	37.46 ± 4.61	49.53 ± 3.92
SHP23	28.91 ± 1.55	56.05 ± 4.99	>100.00	42.25 ± 6.69	57.32 ± 5.46
SHP24	43.20 ± 2.12	49.74 ± 2.93	47.95 ± 2.35	43.27 ± 3.58	45.56 ± 4.73
SHP25	28.03 ± 0.98	18.29 ± 1.88	17.5 ± 1.21	23.46 ± 2.06	25.45 ± 2.96
SHP26	31.22 ± 3.11	20.33 ± 1.75	21.67 ± 2.04	19.22 ± 3.12	21.55 ± 3.35
SHP27	68.88 ± 4.55	14.58 ± 0.74	39.62 ± 3.42	49.23 ± 4.23	43.91 ± 5.87
SHP28	24.65 ± 3.22	24.51 ± 3.31	27.75 ± 1.78	13.39 ± 2.65	18.65 ± 1.54
SHP29	43.46 ± 5.49	70.80 ± 7.83	69.85 ± 5.92	34.47 ± 5.42	45.78 ± 5.43
CX4945 (positive control)	26.28 ± 2.33	15.5 ± 0.91	18.72 ± 1.14	13.56 ± 1.76	12.76 ± 0.89

SHP25 and **SHP26**, showed comparable activity against five cancer cell lines to the positive control. However, several compounds with potent CK2 inhibitory effect, such as **SHP19** and **SHP29**, only showed moderate antiproliferative activities. This may be explained by the unpleasant physicochemical properties such as solubility and cell permeability. As a consequence, further optimization will be focused on improving the druglike abilities of these compounds.

DISCUSSION

When analyzing the binding mode of our compound with CK2, we can observe an obvious polar area mainly consisted of Lys68 and Asp175 (the blue and red surfaces, respectively, Figure 7), two residues that are reported to be significant in the recognition of inhibitors by forming polar interactions. For instance, the carboxic group of CX-4945 forms several important H-bonds with Asp175 and water molecules around it. Removing or changing to other groups leads to the dramatically decrease of the

dx.doi.org/10.1021/ci400114f | J. Chem. Inf. Model. 2013, 53, 2093−2102

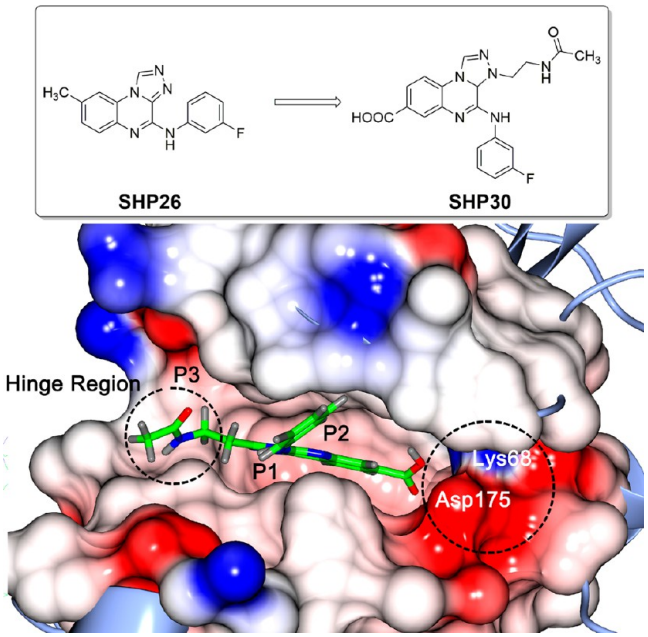

Figure 7. The binding pattern analysis of compound **SHP30** with CK2. Gold 5.1 was used to carry out the molecular docking, and the data were displayed by CCP4MG. Compounds were shown as cylinders. The electrostatic potential surface was added to the active site around the compounds.

activity.[35] The polar interactions between Lys68 and pyrazolo-[1,5-a][1,3,5]triazines compounds are crucial for the intermolecular recognition.[32] For our compounds, although the scaffold fits well to the active site, the inhibitory activities are not as potent as CX-4945 (Table 2). Considering the chemical and molecular shape similarity between our compounds and CX-4945, the loss of polar contacts may be the main reason that causes the decrease of binding affinity. Thus, introduction of polar fragments such as carboxyl, methanesulfonamide, methylguanidine, and hydroximic acid may improve the intermolecular recognition between the compounds and CK2.

Besides, the docking study reveals that our compounds do not contact with the hinge region of CK2, which is formed by residues Glu114, His115, Val116, Asn117, Asn118, etc. The hinge region has been reported to play a crucial role in the intermolecular recognition between kinases and their inhibitors. Thus, interactions with the hinge region can improve the binding affinity of this series of compounds; this may be fulfilled by introducing polar side chains to the scaffold B.

Compound **SHP30** is designed from **SHP26**, a compound showing promising activity in not only target-based level but also cell-based level. It was docked into the active site of CK2. **SHP30** forms hydrogen bonds with Lys68 and several water molecules around polar region using its carboxyl group (Figure 7), The strong polar contacts help the stable binding of **SHP30** to CK2. The amide side chain locates closely to the surface of hinge region residues (Figure 7) as expected and formed hydrogen bonds to the hinge region residues. The docking results provide us the molecular optimization strategy, and the synthesis and biological evaluation of the compound will be carried out in the future.

CONCLUSIONS

Combining the shape-based virtual screening and the structure-based molecular modification, here we report a series of novel tricyclic compounds as CK2 inhibitors. The shape-based screening model was built using the ROCS method, based on CX-4945, an CK2 inhibitor now entering the phase II clinical trial. The model was then applied to virtually screen the Topscience database, resulting in the lead compound **SHP01**, a compound with [1,2,4]triazolo[4,3-c]quinazolin scaffold. To discover more compounds with similar structures to **SHP01**, a ROCS model was then generated on the basis of **SHP01** and then the second-round virtual screening was carried out. The resulting hits were further filtered by chemical similarity analysis, enriching molecules with similar scaffold to **SHP01**. The finally retained compounds (**SHP01**−**SHP29**) were purchased from Topscience and evaluated for their anti-CK2 efficacy as well as antiproliferative activity in multiple cancer cell lines. Compounds with the [1,2,4]triazolo[4,3-a]quinoxalin core exhibited promising inhibitory activities against not only the target but also the cancer cell lines. We also discussed the molecular optimization strategy of these compounds. Our work presented here provided novel leads for the development of CK2 inhibitors. Besides, compared to other virtual screening methods, our workflow supplies a high efficient strategy in the identification of novel CK2 inhibitors and can be applied for other therapeutic targets.

EXPERIMENTAL SECTION

Computational Calculation. *Creation of Topscience Database and Designed Molecules.* The Topscience database file was downloaded from the official Web site. Multiple conformations of the database were generated by using OMEGA (Open Eye Scientific Software) with the following parameters: number of allowed conformations (nconfs) = 400, Ewindow = 10 kcal/mol, and root-mean-square distance (RMS) = 0.5 Å. The Merck Molecular Force Field 94 (MMFF94) was used during the conformation generation. Ewindow is the value used to discard high-energy conformations. The maximum allowed conformations per compound was set to 400 to ensure complete conformational coverage.[53]

The designed derivatives were constructed by using molecular modeling software package SYBYL-X 1.0. The Gasteiger−Hückel method was used to calculate partial atomic charges. Tripos force field with a distance-dependent dielectric and the Powell conjugate gradient algorithm (convergence criterion of 0.005 kcal/mol/M) was applied to do the energy minimizations in 2000 steps.

Creation of the ROCS Model and the Virtual Screens Based on It. The shape-based pharmacophore model used in further virtual screening was generated by employing ROCS. CX-4945 was used as a template molecule. The algorithm is based on the idea that the molecular shape of compounds is similar if the molecules overlay well and any volume mismatch results from shape dissimilarity. ROCS maximizes the rigid body overlap of the molecular Gaussian functions and therefore the shared volume between a query molecule and a conformation of a database molecule. For the superimposition of molecules, a smooth Gaussian function is used to represent the molecular volume. Subsequently, the overlay of the molecules is corrected by simple matching of chemical functionalities.[54]

Virtual screenings were then performed based on the query model of CX-4945. The ROCS program was used to carry out the virtual screens. The parameters for the ROCS run were set as follows: rankby = combo and besthits = 1. In this screen, ROCS compares database compounds and CX-4945 by aligning the compounds and calculating the similarities including their volumes and chemical features. The similarity is represented by

dx.doi.org/10.1021/ci400114f | J. Chem. Inf. Model. 2013, 53, 2093−2102

a combo score, ranging from 0 to 2. If the combo score is close to 2, then the molecules have an excellent shape and chemical-feature match; while values close to 0 imply a poor shape and chemical-feature match. The screening score for a particular database compound was set to the maximum combo score between the database compound and CX-4945. Finally, 29 compounds were retained and purchased from the Topscience database with purity >95% (liquid chromatography−mass spectrometry, LCMS).

Molecular Docking. The molecular docking accuracy was first evaluated by programs based on different algorithms, including CDOCKER and Ligandfit implemented in Discovery studio 3.0 (DS), GOLD 5.1, Glide in Schrodinger 2010, and Oedocking within Openeye. CX-4945 from the cocrystal structure (PDB code: 3PE1) was separated and then redocked into the binding site of CK2. The docked conformation was compared to its bound counterpart, and the root-mean-square deviation (RMSD) value was calculated in DS. Gold 5.1 that generated conformation with the lowest RMSD was selected for further docking study.

GOLD uses a powerful genetic algorithm (GA) method for conformation search and docking.[55] As one of the most successful and widely used docking programs, GOLD was tested on a data set of over 300 complexes extracted from the PDB and succeeded in more than 70% of the cases in reproducing the bound conformation of the ligand obtained from experiment.[56] In the present study, the binding site was defined by carefully analyzing the protein−ligand interactions between CK2 and CX-4945. Our previous study has summarized the binding modes of 23 CK2 cocystal structures and has shown that Val53, Val66, Lys68, Val116, Asn118, Ile174, and Asp175 were very important for the ligand binding.[57] Thus, these residues of CK2 were defined as binding sites. Residues around the original ligand (radius 6.5 Å) were also included in the active site. As water molecules have been reported to play a crucial role in the interactions between CK2 and its ligands, all water molecules were retained and hydrogen atoms were added to the whole protein structure. Docking studies were performed using the standard default settings with 10 GA runs on each molecule. For each of the GA runs, a maximum of 125000 operations were performed. With respect to ligand flexibility special care has been taken by including options such as flipping of ring corners, amides, pyramidal nitrogens, secondary and tertiary amines, and rotation of carboxylate groups as well as torsion angle distribution and postprocess rotatable bonds as default. The annealing parameters were used as default cutoff values of 3.0 Å for hydrogen bonds and 4.0 Å for van der Waals interactions. Hydrophobic fitting points were calculated to facilitate the correct starting orientation of the compound for docking by placing the hydrophobic atoms appropriately in the corresponding areas of the active site. When the top three solutions attained RMSD values within 1.5 Å, docking was terminated. Goldscore, a scoring function of the software, is a dimensionless fitness value that takes into account the intra- and intermolecular hydrogen bonding interaction energy, van der Waals energy, and ligand torsion energy.

ClogP Calculation of the Designed Compounds. The physicochemical property CLogP of the designed compounds was calculated by Chemaxon MarvinSketch 5.10.0.[58] The weighted method was used, and all the parameters were set as default.

Biological Test. *Measurement of CK2 Inhibitory Effects of the Screened out Compounds.* Measurement of CK2 activity treated with various inhibitors was carried out by a method previously reported,[57] employing a CK2 assay kit (MBL International, Woburn, MA). Briefly, in a 96-well recombinant full-length p53-coated plate, 10 μL of the positive control containing 20 milliunits/10 μL CK2 was incubated with 10 μL of tested samples and 80 μL of kinase reaction buffer (containing 20X adenosine triphosphate, ATP) for 30 min at 30 °C. Then, the wells were thoroughly washed with Washing Buffer. 100 μL of horseradish peroxidase (HRP) conjugated Detection Antibody TK-4D4 was added into each well. After incubation at room temperature for 60 min, 100 μL of Substrate Reagent was added to each well and incubated at room temperature for 15 min. Finally, 100 μL of Stop Solution containing 3,3′,5,5′-tetramethylbenzidine (TMB) was added to each well, and the absorbance was read by Varioskan spectrofluorometer and spectrophotometer (Thermo, Waltham, MA) at dual wavelengths of 450/540 nm.

Antiproliferation Activity. Cell viabilities were measured by a colorimetric assay using 3-(4,5-dimethylthiaz-ol-2-yl)-2,5-diphenyltetrazoliumbromide (MTT, Sigma, St. Louis, MO) as described previously. Experiments were carried out in triplicate in a parallel manner for each concentration of target compounds, and the results were presented as mean ± SE. Control cells were given only culture media. After incubation for 48 h, absorbance (A) was measured at 570 nm. The survival ratio (%) was calculated using the following equation: survival ratio (%) = $(A_{treatment}/A_{control}) \times 100\%$. IC_{50} was taken as the concentration that caused 50% inhibition of cell viabilities and calculated by the Graphpad 5.0 software.

■ ASSOCIATED CONTENT

Supporting Information

Figure S1: the conformation comparasion of CX-4945 docked by different programs. Table S1: the redocking results of CX-4945 to CK2 by different programs. This material is available free of charge via the Internet at http://pubs.acs.org.

■ AUTHOR INFORMATION

Corresponding Author

*Phone/Fax: +86-25-83271216. E-mail: zhangxiaojin@outlook.com. Corresponding author address: Department of Organic Chemistry, School of Science, China Pharmaceutical University, Nanjing 210009, China (X.Z.). Phone/Fax: +86-535-6902143. E-mail: lzl_0_0@126.com. Corresponding author address: School of Pharmacy, Yantai University, Yantai 264005, China (Z.L.). Phone/Fax: +86-25-83271351. E-mail: youqidong@gmail.com. Corresponding author address: State Key Laboratory of Natural Medicines & Jiangsu Key Laboratory of DrugDesign and Optimization, China Pharmaceutical University, Nanjing 210009, China (Q.Y.).

Notes

The authors declare no competing financial interest.

■ ACKNOWLEDGMENTS

Funding of this research is provided by the project 81230078 (key program), 81202463 (youth foundation program), and 91129732 (general program) of the National Natural Science Foundation of China, Program of State Key Laboratory of Natural Medicines, China Pharmaceutical University (No. JKGQ201103), 2012AA020301 of 863 program, 2010ZX09401-401 and 2009ZX09501-003 of the National Major Science and Technology Project of China (Innovation

and Development of New Drugs). We also thank OpenEye (Santa Fe, NM, USA) and ChemAxon (Los Angeles, CA, USA) for providing licenses for their software.

■ ABBREVIATIONS

CK2, protein kinase CK2; ROCS, rapid overlay of chemical structures; PDB, protein data bank; FCFP_6, Functional-Class Fingerprints_6; MMFF94, Merck Molecular Force Field 94; DS, Discovery studio; LCMS, liquid chromatography−mass spectrometry; RMSD, root-mean-square deviation; GA, genetic algorithm; TMB, 3,3′,5,5′-tetramethylbenzidine; ATP, adenosine triphosphate; MTT, 3-(4,5-dimethylthiaz-ol-2-yl)-2,5-diphenyltetrazoliumbromide

■ REFERENCES

(1) Pagano, M. A.; Cesaro, L.; Meggio, F.; Pinna, L. A. Protein kinase CK2: a newcomer in the "druggable kinome. *Biochem. Soc. Trans.* **2006**, *34*, 1303−1306.

(2) Duncan, J. S.; Litchfield, D. W. Too much of a good thing: the role of protein kinase CK2 in tumorigenesis and prospects for therapeutic inhibition of CK2. *Biochim. Biophys. Acta* **2007**, *1784*, 33−47.

(3) Meggio, F.; Pinna, L. A. One-thousand-and-one substrates of protein kinase CK2? *FASEB J.* **2003**, *17*, 349−368.

(4) Niefind, K.; Guerra, B.; Ermakowa, I.; Issinger, O. G. Crystal structure of human protein kinase CK2: insights into basic properties of the CK2 holoenzyme. *EMBO J.* **2001**, *20*, 5320−5331.

(5) Ahmad, K. A.; Wang, G.; Unger, G.; Slaton, J.; Ahmed, K. Protein kinase CK2; a key suppressor of apoptosis. *Adv. Enzyme Regul.* **2008**, *48*, 179−187.

(6) Guerra, B.; Issinger, O. Protein kinase CK2 in human diseases. *Curr. Med. Chem.* **2008**, *15*, 1870−1886.

(7) Faust, R. A.; Tawfic, S.; Davis, A. T.; Bubash, L. A.; Ahmed, K. Antisense oligonucleotides against protein kinase CK2-alpha inhibit growth of squamous cell carcinoma of the head and neck in vitro. *Head Neck* **2000**, *22*, 341−346.

(8) Drygin, D.; Ho, C. B.; Omori, M.; Bliesath, J.; Proffitt, C.; Rice, R.; Siddiqui-Jain, A.; O'Brien, S.; Padgett, C.; Lim, J. K.; Anderes, K.; Rice, W. G.; Ryckman, D. Protein kinase CK2 modulates IL-6 expression in inflammatory breast cancer. *Biochem. Biophys. Res. Commun.* **2011**, *415*, 163−7.

(9) Landesman-Bollag, E.; Romieu-Mourez, R.; Song, D. H.; Sonenshein, G. E.; Cardiff, R. D.; Seldin, D. C. Protein kinase CK2 in mammary gland tumorigenesis. *Oncogene* **2001**, *20*, 3247−3257.

(10) Pistorius, K.; Seitz, G.; Remberger, K.; Issinger, O. G. Differential CKII activities in human colorectal mucosa, adenomas and carcinomas. *Onkologie* **1991**, *14*, 256−260.

(11) Stalter, G.; Siemer, S.; Becht, E.; Ziegler, M.; Remberger, K.; Issinger, O. G. Asymmetric expression of protein kinase CK2 subunits in human kidney tumors. *Biochem. Biophys. Res. Commun.* **1994**, *202*, 141−147.

(12) O-charoenrat, P.; Rusch, V.; Talbot, S. G.; Sarkaria, I.; Viale, A.; Socci, N.; Ngai, I.; Rao, P.; Singh, B. Casein kinase II alpha subunit and C1-inhibitor are independent predictors of outcome in patients with squamous cell carcinoma of the lung. *Clin. Cancer Res.* **2004**, *10*, 5792−5803.

(13) Kim, J. S.; Eom, J. I.; Cheong, J. W.; Choi, A. J.; Lee, J. K.; Yang, W. I.; Min, Y. H. Protein kinase CK2alpha as an unfavorable prognostic marker and novel therapeutic target in acute myeloid leukemia. *Clin. Cancer Res.* **2007**, *13*, 1019−1028.

(14) Laramas, M.; Pasquier, D.; Filhol, O.; Ringeisen, F.; Descotes, J. L.; Cochet, C. Nuclear localization of protein kinase CK2 catalytic subunit (CK2alpha) is associated with poor prognostic factors in human prostate cancer. *Eur. J. Cancer* **2007**, *43*, 928−934.

(15) Luo, J.; Solimini, N. L.; Elledge, S. J. Principles of cancer therapy: oncogene and non-oncogene addiction. *Cell* **2009**, *136*, 823−837.

(16) Trembley, J. H.; Chen, Z.; Unger, G.; Slaton, J.; Kren, B. T.; Van Waes, C.; Ahmed, K. Emergence of protein kinase CK2 as a key target in cancer therapy. *Biofactors* **2010**, *36*, 187−95.

(17) Kluetzman, K. S.; Thomas, R. M.; Nechamen, C. A.; Dias, J. A. Decreased degradation of internalized follicle-stimulating hormone caused by mutation of aspartic acid 6.30(550) in a protein kinase-CK2 consensus sequence in the third intracellular loop of human follicle-stimulating hormone receptor. *Biol. Reprod.* **2011**, *84*, 1154−63.

(18) Pagano, M. A.; Bain, J.; Kazimierczuk, Z.; Sarno, S.; Ruzzene, M.; Di Maira, G.; Elliott, M.; Orzeszko, A.; Cozza, G.; Meggio, F.; Pinna, L. A. The selectivity of inhibitors of protein kinase CK2. An update. *Biochem. J.* **2008**, *415*, 353−365.

(19) Zandomeni, R. Z.; Zandomeni, M. C.; Shugar, D.; Weinmann, R. Casein kinase type II is involved in the inhibition by 5,6-dichloro-1-beta-D-ribofuranosylbenzimidazole of specific RNA polymerase II transcription. *J. Biol. Chem.* **1986**, *261*, 3414−3419.

(20) Raaf, J.; Klopffleisch, K.; Issinger, O. G.; Niefind, K. The catalytic subunit of human protein kinase CK2 structurally deviates from its maize homologue in complex with the nucleotide competitive inhibitor emodin. *J. Mol. Biol.* **2008**, *377*, 1−8.

(21) Critchfield, J. W.; Coligan, J. E.; Folks, T. M.; Butera, S. T. Casein kinase II is a selective target of HIV-1 transcriptional inhibitors. *Proc. Natl. Acad. Sci. U.S.A.* **1997**, *94*, 6110−6115.

(22) Cozza, G.; Bonvini, P.; Zorzi, E.; Poletto, G.; Pagano, M. A.; Sarno, S.; Donella-Deana, A.; Zagotto, G.; Rosolen, A.; Pinna, L. A.; Meggio, F.; Moro, S. Identification of ellagic acid as potent inhibitor of protein kinase CK2: a successful example of a virtual screening application. *J. Med. Chem.* **2006**, *49*, 2363−2366.

(23) Pagano, M. A.; Andrzejewska, M.; Ruzzene, M.; Sarno, S.; Cesaro, L.; Bain, J.; Elliott, M.; Meggio, F.; Kazimierczuk, Z.; Pinna, L. A. Optimization of protein kinase CK2 inhibitors derived from 4,5,6,7-tetrabromobenzimidazole. *J. Med. Chem.* **2004**, *47*, 6239−6247.

(24) Ruzzene, M.; Penzo, D.; Pinna, L. A. Protein kinase CK2 inhibitor 4,5,6,7-tetrabromobenzotriazole (TBB) induces apoptosis and caspase-dependent degradation of haematopoietic lineage cell-specific protein 1 (HS1) in Jurkat cells. *Biochem. J.* **2002**, *364*, 41−47.

(25) Zien, P.; Bretner, M.; Zastapilo, K.; Szyszka, R.; Shugar, D. Selectivity of 4,5,6,7-tetrabromobenzimidazole as an ATP-competitive potent inhibitor of protein kinase CK2 from various sources. *Biochem. Biophys. Res. Commun.* **2003**, *306*, 129−133.

(26) Sarno, S.; Reddy, H.; Meggio, F.; Ruzzene, M.; Davies, S. P.; Donella-Deana, A.; Shugar, D.; Pinna, L. A. Selectivity of 4,5,6,7-tetrabromobenzotriazole, an ATP site-directed inhibitor of protein kinase CK2 ('casein kinase-2'). *FEBS Lett.* **2001**, *496*, 44−48.

(27) Sarno, S.; Pinna, L. A. Protein kinase CK2 as a druggable target. *Mol. Biosyst.* **2008**, *4*, 889−894.

(28) DePierre, J. W. Mammalian Toxicity of Organic Compounds of Bromine and Iodine. In *Organic Bromine and Iodine Compounds*; Neilson, A. H., Ed.; Springer-Verlag: Berlin-Heidelberg-New York, 2003; Vol. 3*R*, pp 221−232.

(29) Vangrevelinghe, E.; Zimmermann, K.; Schoepfer, J.; Portmann, R.; Fabbro, D.; Furet, P. Discovery of a potent and selective protein kinase CK2 inhibitor by high-throughput docking. *J. Med. Chem.* **2003**, *46*, 2656−2662.

(30) Sarno, S.; Ruzzene, M.; Frascella, P.; Pagano, M. A.; Meggio, F.; Zambon, A.; Mazzorana, M.; Di Maira, G.; Lucchini, V.; Pinna, L. A. Development and exploitation of CK2 inhibitors. *Mol. Cell. Biochem.* **2005**, *274*, 69−76.

(31) Nie, Z.; Perretta, C.; Erickson, P.; Margosiak, S.; Lu, J.; Averill, A.; Almassy, R.; Chu, S. Structure-based design and synthesis of novel macrocyclic pyrazolo[1,5-a] [1,3,5]triazine compounds as potent inhibitors of protein kinase CK2 and their anticancer activities. *Bioorg. Med. Chem. Lett.* **2008**, *18*, 619−623.

(32) Nie, Z.; Perretta, C.; Erickson, P.; Margosiak, S.; Almassy, R.; Lu, J.; Averill, A.; Yager, K. M.; Chu, S. Structure-based design, synthesis, and study of pyrazolo[1,5-a][1,3,5]triazine derivatives as potent inhibitors of protein kinase CK2. *Bioorg. Med. Chem. Lett.* **2007**, *17*, 4191−4195.

(33) Zhu, D.; Hensel, J.; Hilgraf, R.; Abbasian, M.; Pornillos, O.; Deyanat-Yazdi, G.; Hua, X. H.; Cox, S. Inhibition of protein kinase CK2 expression and activity blocks tumor cell growth. *Mol. Cell. Biochem.* **2009**, *333*, 159−167.
(34) Prudent, R.; Cochet, C. New protein kinase CK2 inhibitors: jumping out of the catalytic box. *Chem. Biol.* **2009**, *16*, 112−20.
(35) Pierre, F.; Chua, P. C.; O'Brien, S. E.; Siddiqui-Jain, A.; Bourbon, P.; Haddach, M.; Michaux, J.; Nagasawa, J.; Schwaebe, M. K.; Stefan, E.; Vialettes, A.; Whitten, J. P.; Chen, T. K.; Darjania, L.; Stansfield, R.; Anderes, K.; Bliesath, J.; Drygin, D.; Ho, C.; Omori, M.; Proffitt, C.; Streiner, N.; Trent, K.; Rice, W. G.; Ryckman, D. M. Discovery and SAR of 5-(3-chlorophenylamino) benzo[c][2,6]naphthyridine-8-carboxylic acid (CX-4945), the first clinical stage inhibitor of protein kinase CK2 for the treatment of cancer. *J. Med. Chem.* **2011**, *54*, 635−654.
(36) Battistutta, R.; Cozza, G.; Pierre, F.; Papinutto, E.; Lolli, G.; Sarno, S.; O'Brien, S. E.; Siddiqui-Jain, A.; Haddach, M.; Anderes, K.; Ryckman, D. M.; Meggio, F.; Pinna, L. A. Unprecedented selectivity and structural determinants of a new class of protein kinase CK2 inhibitors in clinical trials for the treatment of cancer. *Biochemistry* **2011**, *50*, 8478−8488.
(37) For the clinical study information see the following Web page: http://www.cylenepharma.com/pipeline/ck2-program (accessed 2013/01/24).
(38) Chiang, Y. K.; Kuo, C. C.; Wu, Y. S.; Chen, C. T.; Coumar, M. S.; Wu, J. S.; Hsieh, H. P.; Chang, C. Y.; Jseng, H. Y.; Wu, M. H.; Leou, J. S.; Song, J. S.; Chang, J. Y.; Lyu, P. C.; Chao, Y. S.; Wu, S. Y. Generation of ligand-based pharmacophore model and virtual screening for identification of novel tubulin inhibitors with potent anticancer activity. *J. Med. Chem.* **2009**, *52*, 4221−4233.
(39) Sirci, F.; Goracci, L.; Rodriguez, D.; van Muijlwijk-Koezen, J.; Gutierrez-de-Teran, H.; Mannhold, R. Ligand-, structure- and pharmacophore-based molecular fingerprints: a case study on adenosine A(1), A (2A), A (2B), and A (3) receptor antagonists. *J. Comput.-Aided Mol. Des.* **2012**, *26*, 1247−1266.
(40) Thangapandian, S.; John, S.; Sakkiah, S.; Lee, K. W. Ligand and structure based pharmacophore modeling to facilitate novel histone deacetylase 8 inhibitor design. *Eur. J. Med. Chem.* **2010**, *45*, 4409−17.
(41) Purushottamachar, P.; Khandelwal, A.; Chopra, P.; Maheshwari, N.; Gediya, L. K.; Vasaitis, T. S.; Bruno, R. D.; Clement, O. O.; Njar, V. C. First pharmacophore-based identification of androgen receptor down-regulating agents: discovery of potent anti-prostate cancer agents. *Bioorg. Med. Chem.* **2007**, *15*, 3413−3421.
(42) Sala, E.; Guasch, L.; Iwaszkiewicz, J.; Mulero, M.; Salvado, M. J.; Blade, C.; Ceballos, M.; Valls, C.; Zoete, V.; Grosdidier, A.; Garcia-Vallve, S.; Michielin, O.; Pujadas, G. Identification of human IKK-2 inhibitors of natural origin (Part II): in silico prediction of IKK-2 inhibitors in natural extracts with known anti-inflammatory activity. *Eur. J. Med. Chem.* **2011**, *46*, 6098−6103.
(43) Chen, J. J.; Liu, T. L.; Yang, L. J.; Li, L. L.; Wei, Y. Q.; Yang, S. Y. Pharmacophore modeling and virtual screening studies of checkpoint kinase 1 inhibitors. *Chem. Pharm. Bull.* **2009**, *57*, 704−709.
(44) *OMEGA*, 2.4.6; OpenEye Scientific Software: Santa Fe, NM, 2012.
(45) *ROCS*, 3.1.2; OpenEye Scientific Software: Santa Fe, NM, 2012.
(46) Tawa, G. J.; Baber, J. C.; Humblet, C. Computation of 3D queries for ROCS based virtual screens. *J. Comput.-Aided Mol. Des.* **2009**, *23*, 853−68.
(47) Rush, T. S.; Grant, J. A.; Mosyak, L.; Nicholls, A. A shape-based 3-D scaffold hopping method and its application to a bacterial protein-protein interaction. *J. Med. Chem.* **2005**, *48*, 1489−1495.
(48) Moffat, K.; Gillet, V. J.; Whittle, M.; Bravi, G.; Leach, A. R. A comparison of field-based similarity searching methods: CatShape, FBSS, and ROCS. *J. Chem. Inf. Model.* **2008**, *48*, 719−729.
(49) Kirchmair, J.; Distinto, S.; Markt, P.; Schuster, D.; Spitzer, G. M.; Liedl, K. R.; Wolber, G. How to optimize shape-based virtual screening: choosing the right query and including chemical information. *J. Chem. Inf. Model.* **2009**, *49*, 678−692.
(50) Schuster, D.; Spetea, M.; Music, M.; Rief, S.; Fink, M.; Kirchmair, J.; Schutz, J.; Wolber, G.; Langer, T.; Stuppner, H.; Schmidhammer, H.; Rollinger, J. M. Morphinans and isoquinolines: acetylcholinesterase inhibition, pharmacophore modeling, and interaction with opioid receptors. *Bioorg. Med. Chem.* **2010**, *18*, 5071−5080.
(51) Liu, R.; Zhou, D. Using molecular fingerprint as descriptors in the QSPR study of lipophilicity. *J. Chem. Inf. Model.* **2008**, *48*, 542−549.
(52) Xue, L.; Godden, J. W.; Stahura, F. L.; Bajorath, J. Design and evaluation of a molecular fingerprint involving the transformation of property descriptor values into a binary classification scheme. *J. Chem. Inf. Comput. Sci.* **2003**, *43*, 1151−1157.
(53) AbdulHameed, M. D.; Chaudhury, S.; Singh, N.; Sun, H.; Wallqvist, A.; Tawa, G. J. Exploring polypharmacology using a ROCS-based target fishing approach. *J. Chem. Inf. Model.* **2012**, *52*, 492−505.
(54) Hawkins, P. C.; Skillman, A. G.; Nicholls, A. Comparison of shape-matching and docking as virtual screening tools. *J. Med. Chem.* **2007**, *50*, 74−782.
(55) Jones, G.; Willett, P.; Glen, R. C.; Leach, A. R.; Taylor, R. Development and validation of a genetic algorithm for flexible docking. *J. Mol. Biol.* **1997**, *267*, 727−748.
(56) Nissink, J. W.; Murray, C.; Hartshorn, M.; Verdonk, M. L.; Cole, J. C.; Taylor, R. A new test set for validating predictions of protein-ligand interaction. *Proteins* **2002**, *49*, 457−471.
(57) Sun, H. P.; Zhu, J.; Chen, F. H.; You, Q. D. Structure-based pharmacophore modeling from multicomplex: a comprehensive pharmacophore generation of protein kinase CK2 and virtual screening based on it for novel inhibitors. *Mol. Inf.* **2011**, *30*, 579−592.
(58) *MarvinSketch* 5.10.0; ChemAxon Software: Los Angeles, CA, 2012.